
Since January 2020 Elsevier has created a COVID-19 resource centre with free information in English and Mandarin on the novel coronavirus COVID-19. The COVID-19 resource centre is hosted on Elsevier Connect, the company's public news and information website.

Analytical Biochemistry 661 (2023) 114983

Contents lists available at ScienceDirect

Analytical Biochemistry

journal homepage: www.elsevier.com/locate/yabio

# A duplex-specific nuclease based electrochemical biosensor for the assay of SARS-CoV-2 RdRp RNA

Ke Zhou [a], Jing Dai [b,*]

[a] Department of Laboratory Medicine, Jiangyin Hospital of Traditional Chinese Medicine (Jiangyin Hospital Affiliated to Nanjing University of Chinese Medicine), Jiangyin, Jiangsu, China
[b] Department of Laboratory Medicine, Jiangyin Fifth People's Hospital, Jiangyin, Jiangsu, China

ARTICLE INFO

*Keywords:*
SARS-CoV-2
DSN
Electrochemistry
2-OMe-RNA

ABSTRACT

We present a method for severe acute respiratory syndrome coronavirus 2 (SARS-CoV-2) detection based on the dual amplification effect of duplex-specific nuclease (DSN). In this scheme, we cleverly employed a 2-OMe-RNA modified DNA to prevent hairpin nucleic acid from being digested by DSN. The target RNA and 2-OMe-RNA are released when DSN cleaves just the double-stranded RNA/hairpin nucleic acid DNA. The target RNA then forms a circular reaction when it hybridizes with another hairpin nucleic acid. Simultaneously, the released target 2-OMe-RNA turns on the hairpin DNA2 on the electrode surface, and when the DSN cleaves the DNA in the hairpin DNA2/2-OMe-RNA duplex, the 2-OMe-RNA is released and hybridized with the other hairpin DNA2. The hairpin DNA2 on the electrode surface is split off after many cycles, exposing the gold electrode surface. As a consequence, there is more $K_4[Fe(CN)_6]/K_3[Fe(CN)_6]$ redox near to the electrode surface, and the electrochemical signal increases. As a result, the change in electrochemical signal may be used to calculate the quantity of RNA that has to be measured. The protocol has good sensitivity in the detection of SARS-CoV-2: the detection limit reached 21.69 aM. This protocol provides an effective solution for the highly sensitive screening of SARS-CoV-2.

## 1. Introduction

Since December 2019, a global outbreak of respiratory disease with fever, malaise, and dry cough as the main symptoms has been occurring one after another, and the pathogen was later identified by laboratory isolation as a new coronavirus [1–4]. Pneumonia caused by coronavirus disease (COVID-19) infection, also known as COVID-19 pneumonia, affects people of all ages, and the virus has spread rapidly worldwide in the last two years. The case will be confirmed using polymerase chain reaction (qPCR) to identify new coronaviruses or sequencing of the viral gene with a high degree of resemblance to a known novel coronavirus. The gold standard for validating the diagnosis of neo-coronavirus is pathogenic testing. qPCR nucleic acid testing is the most extensively utilized technique in identifying neo-coronavirus at this time due to its lengthy test cycle, tedious processes, and relatively high technical requirements for testers [5–7]. As a result, new approaches for identifying novel coronaviruses are desperately needed. The standard method for identifying severe acute respiratory syndrome coronavirus 2 (SARS-CoV-2) is to convert the virus's genetic material, RNA, to DNA and then do PCR amplification. The lengthy procedures raise the risk of false-negative viral detection. To eliminate false negatives in the test, a straightforward technique for direct viral RNA detection is urgently required.

In the field of RNA detection, the primary detection methods commonly used today are Northern blot, quantitative reverse transcription-polymerase chain reaction (RT-qPCR), microarray technology, and optical methods. However, these methods have certain drawbacks: semi-quantitative, complicated pre-treatment, and large labor force [5–7]. Electrochemical biosensors have been widely used in various fields because of their advantages: simple operation, high sensitivity, fast analysis, low detection cost, and easy miniaturization. It is of interest that some researchers have taken advantage of electrochemical biosensors in combination with isothermal amplification to achieve sensitive and accurate detection of biomolecules. This is due to the following benefits of isothermal amplification: (1) easy operation, (2) significantly improved sensitivity, and (3) improved accuracy of quantitative detection of analytes [5,6,8,9]. Therefore, isothermal amplification electrochemical sensors provide a new idea for detecting

* Corresponding author.
*E-mail address:* 7233178@qq.com (J. Dai).

https://doi.org/10.1016/j.ab.2022.114983
Received 12 September 2022; Received in revised form 26 October 2022; Accepted 8 November 2022
Available online 21 November 2022

RNA.

The short length and low quantity of RNA fragments, as well as sequence similarity across family members, make detection problematic [10]. Researchers have devised a number of signal amplification solutions to address this issue, including real-time quantitative fluorescence polymerase chain reaction (qRT-PCR), hybridization chain reaction (HCR), rolling circle amplification (RCA), and duplex-specific nuclease (DSN)-assisted target loop amplification. DSN-assisted target-loop amplification has been employed as a simple and effective RNA detection approach among them [11]. DSN had a high predilection for DNA strands in double-stranded nucleic acids, and although it did not cleave RNA, it did cleave DNA successfully [12,13]. However, some of the amplification methodologies discussed above (such as qRT-PCR, DSN, and others) frequently target just a single RNA for signal amplification, making it difficult to identify several RNA signals in the same system. As a result, developing analytical tools that can amplify and distinguish numerous RNA signals is critical.

We present a DSN-amplification-based approach for SARS-CoV-2 nucleic acid detection that is inspired by DSN's isothermal amplification capacity paired with the benefits of electrochemistry. A little quantity of target RNA, following amplification, produces a high number of cleaved DNA probes, which may then be identified by electrochemistry for sensitive detection of the RNA to be tested, thanks to DSN-assisted amplification and electrochemical signaling.

## 2. Experimental section

### 2.1. Reagents

Sigma-Aldrich Inc. provided the tris(2-carboxyethyl) phosphine hydrochloride (TCEP) and diethylpyrocarbonate (DEPC) (St. Louis, Missouri, USA). The nucleic acid chain sequences used in the studies were bought from Genscript Biotech Ltd. (Nanjing, China), and the sequence is listed in Table S1. Newbornco Co., Ltd provided double strand-specific nuclease (DSN) (Shenzhen, China). Before usage, the RNAs were diluted to the desired concentration using DEPC-treated water. For Hairpin DNA1 and Hairpin DNA2, 10 mM HEPES (with 100 mM NaCl and 25 mM KCl) was utilized. All investigations utilized DEPC-treated deionized water.

### 2.2. Fabrication of the electrochemical biosensor

To remove organic material from the gold electrode surface (2 mm diameter), it was submerged in a newly made piranha solution (30% $H_2O_2$: $H_2SO_4$ = 1:3) for 5 min, then thoroughly cleaned with double-distilled water. The gold electrodes were then meticulously polished using sandpaper and mirror alumina paste (diameters of 1.0, 0.3, and 0.05 μm, respectively), and then sonicated continuously in ethanol and water for 5 min. Finally, the electrodes were cleaned electrochemically by scanning the potential in 0.5 M $H_2SO_4$ from −0.2 to +1.6 V until reliable cyclic voltammograms were produced. The gold electrode was then washed completely with ultrapure water and dried under filtered nitrogen.

Hairpin DNA2 was first denatured for 5 min at 95 °C, then slowly cooled to ambient temperature for roughly 4 h. Hairpin DNA2 efficiently generated hairpin structures in this fashion. The hairpin DNA2 solution was then treated with TCEP (1 mM) for 1 h to break down the disulfide bonds, followed by dilution with Tris-HCl buffer (50 mM, pH 7.4, 10 mM KCl, 5 mM $MgCl_2$, and 0.1 M NaCl) to yield 0.3 μM hairpin DNA2. The hairpin DNA2 was then applied dropwise to the electrode surface for 12 h at 4 °C. S–Au bonding was used to immobilize the hairpin DNA2 on the Au electrode surface. After cleaning the electrode surface with 10 mM PBS (pH 7.4, 0.1 μM NaCl) and drying it with flowing nitrogen, 6 μL of 6-Hydroxy-1-hexanethiol (MCH) solution (1 mM) was placed on the electrode surface for 1 h to fill the pinholes in the DNA2 monolayer. The biosensor was obtained and kept at 4 °C after washing with PBS and drying with pure nitrogen.

### 2.3. Amplification reactions

All assay procedures consist of two consecutive steps. For double-stranded specific nuclease (DSN) amplification, a volume of 50 μL of reaction mixture containing 1× DSN buffer (50 mM Tris-HCl, pH 8.0; 5 mM $MgCl_2$, 1 mM Dithiothreitol (DTT), 10 mM HEPES, 100 mM NaCl, and 25 mM KCl), 0.5 U of DSN (dissolved in 25 mM Tris-HCl and containing 50% glycerol, pH 8.0), 20 U RNase inhibitor, 1 μM Hairpin DNA1, and various concentrations of target RNA.

The above solutions were mixed and incubated for 60 min to allow complete reaction of the DSN-assisted amplification reaction. Control experiments were performed under the same conditions without the addition of the target RNA to be tested. Subsequently, 30 μL of 10 mM EDTA was added to the reaction mixture and incubated for 5 min at 60 °C to activate the DSN enzyme. Next, after the amplification reaction, the solution was added dropwise to the prepared biosensor and reacted at room temperature for 30 min. Electrochemical detection was performed immediately afterward.

### 2.4. Electrochemical assay

To induce a DSN assisted ring-opening reaction on the electrode surface, 6 μL of the aforementioned solution was put onto the biosensor surface for 60 min at room temperature. The electrochemical biosensor was submerged in the solution (5 mM $K_4[Fe(CN)_6]/K_3[Fe(CN)_6]$ (1:1) in PBS (0.1 M KCl, pH 7.4)) for differential pulse voltammetry (DPV) detection after being washed with 10 mM PBS (pH 7.4). The reaction was carried out on a CHI 660E electrochemical workstation (CH Instruments) with a platinum wire counter electrode, an Ag/AgCl electrode as a reference electrode, and a 2 mm diameter gold electrode as a working electrode. The electrochemical scan step potential is 4 mV and the scan range is −0.1 V to +0.6 V.

## 3. Results and discussion

### 3.1. The working principle

Scheme 1 depicts the electrochemical sensor's operation based on the DSN-assisted target recovery signal amplification approach. This method is used to construct hairpin nucleic acids (hairpin DNA1 and hairpin DNA2). The 3′ end of the hairpin DNA1 may be complementarily mated with the 5′ end nucleic acid to produce a double strand; the middle section is the target RNA recognition area. DSN can break dsDNA, hence the hybridized component of the hairpin nucleic acid stem duplex is easily digested by it [11]. Hairpin nucleic acid is modified with 2-OMe-RNA in its stem to avoid a false-positive result. The DSN is unable to cleave 2-OMe-RNA, which differs from DNA by 2-OMe on pentose. Since the DSN does not cleave hairpin DNA1, the biosensor generates a low electrochemical signal in the absence of the target RNA.

Hybridization of the hairpin nucleic acid with the RNA to be tested causes the hairpin nucleic acid to become a substrate for DSN cleavage in the presence of the RNA to be tested. The target RNA and 2-OMe-RNA are released when DSN cleaves just the double-stranded RNA/hairpin nucleic acid DNA. The target RNA then forms a circular reaction when it hybridizes with another hairpin nucleic acid. In theory, a single RNA sequence may cause the cleavage of several hairpin nucleic acids, resulting in more target 2-OMe-RNA.

DSN shows a strong preference for being able to cleave double-stranded DNA (more than 10 base pairs) or DNA in DNA/RNA duplexes. DSN does not cleave single-stranded DNA or single-stranded RNA [11]. For Hairpin DNA2, which we designed, Hairpin DNA2 is likewise not degraded by the DSN enzyme since the double-stranded DNA in the neck has only 8 base pairs. Therefore, only when target 2-OMe-RNA opens the hairpin structure of Hairpin DNA2, it can be

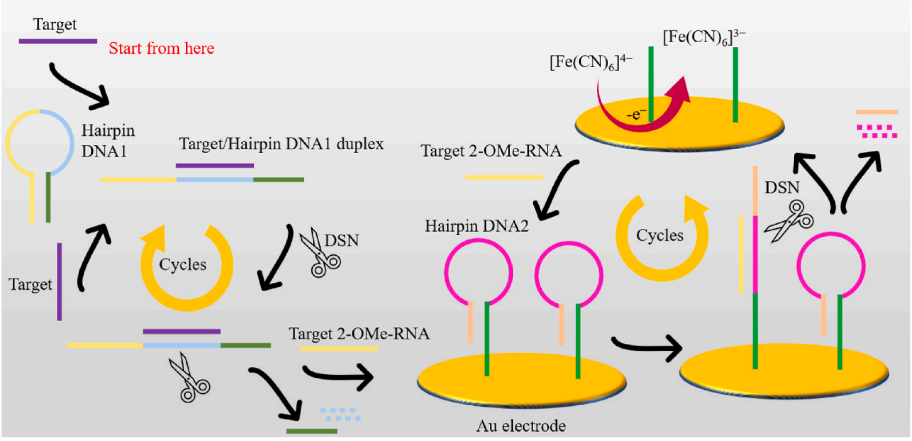


**Scheme 1.** Schematic diagram of the operating principle of an electrochemical sensor based on the DSN-assisted target recovery signal amplification method.

degraded by DSN. Simultaneously, the released target 2-OMe-RNA turns on the hairpin DNA2 (The structure is shown in Figure Fig. S1) on the electrode surface, and when the DSN cleaves the DNA in the hairpin DNA2/2-OMe-RNA duplex, the 2-OMe-RNA is released and hybridized with the other hairpin DNA2. The hairpin DNA2 on the electrode surface is split off after many cycles, exposing the gold electrode surface. As a consequence, there is more $K_4[Fe(CN)_6]/K_3[Fe(CN)_6]$ redox near to the electrode surface, and the electrochemical signal increases. During the electrochemical scan, the $[Fe(CN)_6]^{4-}$ in solution is oxidized to $[Fe(CN)_6]^{3-}$ during the forward scan from its actual potential (−0.1 V) to the termination potential (+0.6 V), generating an oxidation current. As a result, the change in electrochemical signal may be used to calculate the quantity of RNA that has to be measured.

Of course, this strategy has the disadvantage of being cumbersome compared to conventional PCR methods because it does not detect target RNA in a homogeneous system. However, the strategy has the advantages of high sensitivity and high specificity due to the easy separation based on the solid phase system. In addition, the conventional PCR method requires tedious warming up as well as cooling down, while the scheme of this strategy does not require tedious temperature adjustment process and therefore has a greater advantage in terms of stability. Therefore, this strategy has a strong application prospect for clinical detection of SARS-CoV-2 RNA.

### 3.2. Feasibility Study

We evaluated the electrochemical intensity variations under various situations to confirm the feasibility of the quantitative test. The electrochemical changes of the combination of hairpin nucleic acid and DSN (curve b) and without target RNA (curve a) were comparatively modest, as illustrated in Fig. 1A. The electrochemical signal changed very little when 1000 aM of target RNA was added to the aforementioned mixture without DSN (curve d) or DNA1 (curve c). We saw a considerable rise in the alteration of the electrochemical signal when both target RNA (1000 aM) and DSN were present in the solution (curve e). The impact of DSN concentration on this amplification reaction was next investigated, and we discovered that the DPV signal steadily rose with increasing DSN enzyme concentration (Fig. 1B), peaking when we employed 0.5 U DSN for the amplification process. For the following trials, we selected 0.5 U DSN.

Kinetic investigations were carried out to better understand the method's time-dependent signal changes by collecting the values of electrochemical intensity changes at the designated time points following the injection of 10 aM (data points a) and 100 aM (data points b) target RNA. The majority of the electrochemical intensity change values occurred in the first 30 min, as shown in Fig. 1C, and the electrical signal change values of the two RNA samples to be examined stabilized

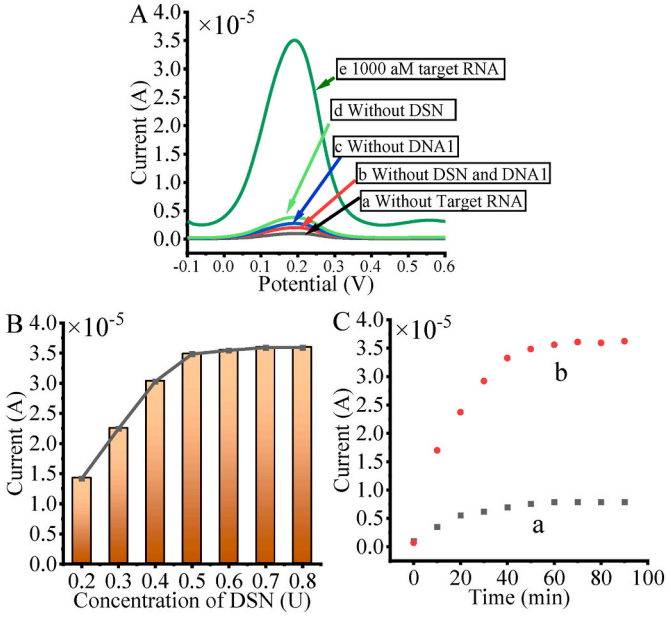


**Fig. 1.** Feasibility Study: (A) Details of the electrochemical signals of different conditions. The differential pulse voltammetry (DPV) curve of duplex-specific nuclease (DSN) and DNA1 (without target RNA) (curve a), 1000 aM target RNA (without DSN and DNA1) (curve b), DSN and 1000 aM target RNA (without DNA1) (curve c), DNA1 and 1000 aM target RNA (without DSN), treated with DNA2 modified electrode (curve d) and DSN, DNA1 and 1000 aM target RNA, treated with DNA2 modified electrode (curve e), respectively. (B) Details of the electrochemical signals at different concentrations of DSN: optimization of DSN concentration at the DSN incubation time of 60 min. (C) Details of the electrochemical signals at different times: Optimization of reaction time of 10 aM (data points a) and 100 aM (data points b) target RNA.

about 50 min. As a result, we used a 50-min reaction time to detect the RNA.

### 3.3. Sensitivity of the biosensor

As shown in Fig. 2A and B, we tested the testing performance of the biosensor employed to analyze various amounts of SARS-CoV-2 RNA. The degree of change in the electrochemical signal was used to profile the concentration of the target SARS-CoV-2 RNA. As shown in Fig. 2B, a rapid increase in DPV intensity followed as the detection range of SARS-CoV-2 RdRp gene concentration gradually increased from 0 aM to 400 aM. Furthermore, the link between DPV intensity and the target SARS-

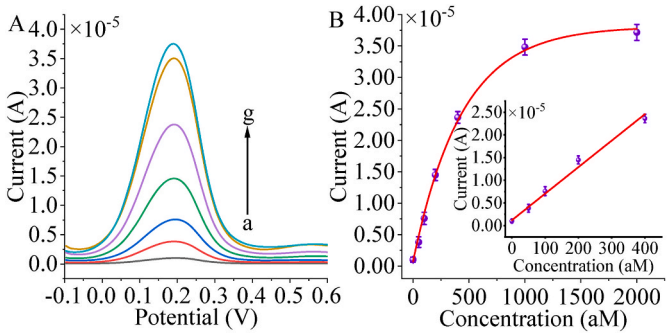


**Fig. 2.** Plot of electrochemical signal values versus SARS-CoV-2 RdRp concentration. (A) Details of the electrochemical current and concentrations of SARS-CoV-2 RNA. The curves a to g correspond to the concentrations of 0 aM (curve a), 50 aM (curve b), 100 aM (curve c), 200 aM (curve d), 400 aM (curve e), 1000 aM (curve f) and 2000 aM (curve g), respectively. (B) Details of the relationship of the differential pulse voltammetry (DPV) value and the concentrations of SARS-CoV-2 RNA. Inset is the linear part of the relationship.

CoV-2 RNA was studied further. The linear equation was $Y = 1.20 \times 10^{-6} + 5.85 \times 10^{-8} X$ ($R^2 = 0.9892$), where Y represents the sample and blank sample DPV values at a certain concentration, and X indicates the concentration of SARS-CoV-2 RNA. We utilized the 3σ/slope approach to get a limit of detection (LOD) of 21.69 aM with this biosensor. The slope is calculated using the linear equation and the standard deviation of 0 aM target RNA. The amplification effect of DSN and the high sensitivity of electrochemistry are responsible for the great test sensitivity. As a result, our approach delivers an effective and ultrasensitive test method for SARS-CoV-2 RdRp gene. Our biosensing system has better or comparable sensitivity than earlier studies (Table 1).

### 3.4. Selectivity of the DSN-based biosensor

To further investigate the selectivity of this DSN amplification-based biosensor, we selected several target RNA analogs (unspecific sequences, RNA1, RNA2, and RNA3 in Table S1) and other virus RNA (SARS-CoV RdRp gene (S1), SARS-CoV-2 E gene (E gene), Bat SARS-related CoV isolate bat-SL-CoVZC45 RdRp (BS gene), Frankfurt 1 RdRp (F gene), and BM48-31/BGR/2008 RdRp (BR gene)) to process this biosensor and detect the DPV signal. Various signal variations of the biosensor are generated when different RNAs (400 aM each) are treated with it. The DPV values of target RNA analogs (unspecific sequences) are shown in Fig. 3. The target RNA has the greatest DPV signal relative to the other RNAs, whereas the other RNAs have no significant electrochemical signal changes. The fact that only SARS-COV-2 RdRp RNA can combine with DNA1 and start the DSN amplification response may explain the outcome of this experiment. As a result, the electrochemical biosensor we built using DSN amplification exhibits high selectivity.

### 3.5. The biosensor assay in pharyngeal swabs

The DSN amplification-based biosensor was used to evaluate SARS-CoV-2 RdRp RNA in pharyngeal swabs in order to see whether it could be applied to actual samples and suit clinical demands. Instead of utilizing reference samples, the SARS-CoV-2 RdRp RNAs (30 aM, 50 aM, 100 aM, 200 aM, and 400 aM, respectively) included in pharyngeal swabs were evaluated using a DSN amplification-based biosensor. We measured the DPV levels after adding various amounts of RNA to the pharyngeal swab solution. Following the experiment, the concentration values of RNA to be evaluated were calculated using the method in section 3.3. The recovery results were computed using the estimated RNA concentration value as well as the added RNA concentration. Table 2 displays the recovery outcomes. These findings indicate that the biosensing method we created may be used to look for SARS-CoV-2 RdRp RNA in pharyngeal swabs. As a result, the analysis strategy we presented for this profiling platform has the potential to be extensively employed in the clinic to investigate SARS-CoV-2 associated RNA in complicated biological materials.

**Table 1**
Comparison of different amplification methods for SARS-CoV-2 assay.

| Method | Target | LOD | Reference |
|---|---|---|---|
| HCR | RdRp gene | 59 aM | [8] |
| DNA walker | RdRP gene | 12.8 aM | [9] |
| Entropy-driven amplification | RdRp gene | 32.8 aM | [5] |
| Real-time optomagnetic | RdRp gene | 0.40 fM | [14] |
| Dual-functional plasmonic | RdRp gene | 0.22 pM | [15] |
| Electrochemical | ORF1ab gene | 0.33 aM | [16] |
| Real-time RT-LAMP/Cas12 | ORF gene | 33.2 aM | [17] |
| RT–LAMP/Cas12 | E and N gene | 16.6 aM | [18] |
| DSN Based Electrochemical Biosensor | RdRp gene | 21.69 aM | This work |

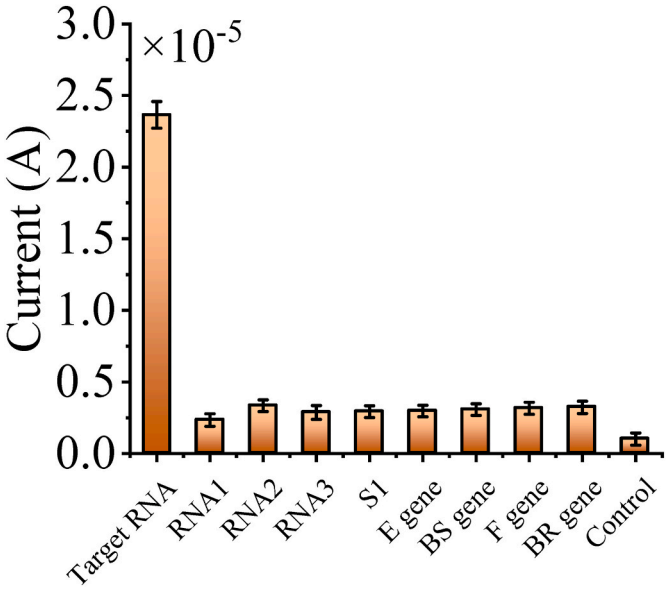


**Fig. 3.** Selectivity of the DSN-based biosensor. The Target RNA has the greatest differential pulse voltammetry (DPV) signal relative to the other RNAs, whereas the other RNAs have no significant electrochemical signal changes.

## 4. Conclusions

In conclusion, we propose to use DSN's amplification capabilities to create an electrochemical biosensor for the detection of SARS-CoV-2 RdRp RNA. We ingeniously used 2-OMe-RNA to prevent DSN from cutting off double-stranded DNA. We used an accession approach with a detection limit of 21.69 aM to identify SARS-CoV-2 RdRp RNA in pharyngeal swabs utilizing this procedure. Furthermore, the detection technique demonstrated high sensitivity in both pharyngeal swabs and buffer solution. The present strategy has the disadvantage of being cumbersome compared to conventional PCR methods because it does not detect target RNA in a homogeneous system. However, due to the advantages of high sensitivity of this strategy and high specificity due to

**Table 2**
Recovery results for the assay of SARS-COV-2 RdRp in pharyngeal swabs.

| Sample number | Added (aM) | Found (aM) | Recovery (%) | RSD (%, n = 3) |
|---|---|---|---|---|
| 1 | 30 | 29.65 | 98.83 | 3.45 |
| 2 | 50 | 51.23 | 102.46 | 4.38 |
| 3 | 100 | 99.46 | 99.46 | 3.78 |
| 4 | 200 | 200.38 | 100.19 | 2.35 |
| 5 | 400 | 407.83 | 101.96 | 3.42 |

easy separation based on the solid phase system detection, this method has a strong application in the clinical detection of SARS-CoV-2 RNA. We think that this biosensor has a lot of promise for detecting SARS-CoV-2.

## Author contributions - Credit

Ke Zhou: Data curation, Formal analysis, Methodology, Software, Writing – original draft; Jing Dai: Writing –review & editing, Supervision, Funding acquisition, Conceptualization.

## Data availability

Data will be made available on request.

## Acknowledgment

This work was supported by the Scientific Instrument Developing Project of the Chinese Academy of Sciences (grant No. YJKYYQ20190080), and the National Key Research and Development Program of China (grant No. 2020YFC0122200).

## Appendix A. Supplementary data

Supplementary data to this article can be found online at https://doi.org/10.1016/j.ab.2022.114983.

## References

[1] K. Zhang, J. Li, Z. Fan, H. Li, J.-J. Xu, Covalent biosensing" enables a one-step, reagent-less, low-cost and highly robust assay of SARS-CoV-2, Chem. Commun. 57 (82) (2021) 10771–10774.
[2] K. Zhang, Z. Fan, Y. Ding, J. Li, H. Li, Thiol-sensitive probe enables dynamic electrochemical assembly of serum protein for detecting SARS-Cov-2 marker protease in clinical samples, Biosens. Bioelectron. 194 (2021), 113579.
[3] B. Yao, J. Zhang, Z. Fan, Y. Ding, B. Zhou, R. Yang, J. Zhao, K. Zhang, Rational engineering of the DNA walker amplification strategy by using a Au@Ti3C2@PEI-Ru(dcbpy)32+ nanocomposite biosensor for detection of the SARS-CoV-2 RdRp gene, ACS Appl. Mater. Interfaces 13 (17) (2021) 19816–19824.
[4] Z. Fan, B. Yao, Y. Ding, J. Zhao, M. Xie, K. Zhang, Entropy-driven amplified electrochemiluminescence biosensor for RdRp gene of SARS-CoV-2 detection with self-assembled DNA tetrahedron scaffolds, Biosens. Bioelectron. 178 (2021), 113015.
[5] K. Zhang, Z. Fan, Y. Ding, S. Zhu, M. Xie, N. Hao, Exploring the entropy-driven amplification reaction and trans-cleavage activity of CRISPR-Cas12a for the development of an electrochemiluminescence biosensor for the detection of the SARS-CoV-2 RdRp gene in real samples and environmental surveillance, Environmental Science: Nano 9 (1) (2022) 162–172.
[6] K. Zhang, Z. Fan, Y. Ding, M. Xie, A pH-engineering regenerative DNA tetrahedron ECL biosensor for the assay of SARS-CoV-2 RdRp gene based on CRISPR/Cas12a trans-activity, Chem. Eng. J. 429 (2022), 132472.
[7] Z. Fan, B. Yao, Y. Ding, D. Xu, J. Zhao, K. Zhang, Rational engineering the DNA tetrahedrons of dual wavelength ratiometric electrochemiluminescence biosensor for high efficient detection of SARS-CoV-2 RdRp gene by using entropy-driven and bipedal DNA walker amplification strategy, Chem. Eng. J. 427 (2022), 131686.
[8] K. Zhang, Z. Fan, Y. Huang, Y. Ding, M. Xie, M. Wang, Hybridization chain reaction circuit-based electrochemiluminescent biosensor for SARS-cov-2 RdRp gene assay, Talanta 240 (2022), 123207.
[9] K. Zhang, Z. Fan, Y. Huang, Y. Ding, M. Xie, A strategy combining 3D-DNA Walker and CRISPR-Cas12a trans-cleavage activity applied to MXene based electrochemiluminescent sensor for SARS-CoV-2 RdRp gene detection, Talanta 236 (2022), 122868.
[10] T. Zhou, M. Huang, J. Lin, R. Huang, D. Xing, High-fidelity CRISPR/Cas13a trans-cleavage-triggered rolling circle amplified DNAzyme for visual profiling of MicroRNA, Anal. Chem. 93 (4) (2021) 2038–2044.
[11] K. Zhang, K. Wang, X. Zhu, F. Xu, M. Xie, Sensitive detection of microRNA in complex biological samples by using two stages DSN-assisted target recycling signal amplification method, Biosens. Bioelectron. 87 (2017) 358–364.
[12] F. Ma, W.-j. Liu, Q. Zhang, C.-y. Zhang, Sensitive detection of microRNAs by duplex specific nuclease-assisted target recycling and pyrene excimer switching, Chem. Commun. 53 (76) (2017) 10596–10599.
[13] X. Lin, C. Zhang, Y. Huang, Z. Zhu, X. Chen, C.J. Yang, Backbone-modified molecular beacons for highly sensitive and selective detection of microRNAs based on duplex specific nuclease signal amplification, Chem. Commun. 49 (65) (2013) 7243–7245.
[14] B. Tian, F. Gao, J. Fock, M. Dufva, M.F. Hansen, Homogeneous circle-to-circle amplification for real-time optomagnetic detection of SARS-CoV-2 RdRp coding sequence, Biosens. Bioelectron. 165 (2020), 112356.
[15] G. Qiu, Z. Gai, Y. Tao, J. Schmitt, G.A. KullakUblick, J. Wang, Dual-functional plasmonic photothermal biosensors for highly accurate severe acute respiratory syndrome coronavirus 2 detection, ACS Nano 14 (5) (2020) 5268–5277.
[16] H. Zhao, F. Liu, W. Xie, T. Zhou, J. OuYang, L. Jin, H. Li, C. Zhao, L. Zhang, J. Wei, Y. Zhang, C. Li, Ultrasensitive supersandwich-type electrochemical sensor for SARS-CoV-2 from the infected COVID-19 patients using a smartphone, Sensor. Actuator. B Chem. 327 (2021), 128899.
[17] Y. Chen, Y. Shi, Y. Chen, Z. Yang, H. Wu, Z. Zhou, J. Li, J. Ping, L. He, H. Shen, Z. Chen, J. Wu, Y. Yu, Y. Zhang, H. Chen, Contamination-free visual detection of SARS-CoV-2 with CRISPR/Cas12a: a promising method in the point-of-care detection, Biosens. Bioelectron. 169 (2020), 112642.
[18] J.P. Broughton, X. Deng, G. Yu, C.L. Fasching, V. Servellita, J. Singh, X. Miao, J. A. Streithorst, A. Granados, A. Sotomayor-Gonzalez, K. Zorn, A. Gopez, E. Hsu, W. Gu, S. Miller, C.-Y. Pan, H. Guevara, D.A. Wadford, J.S. Chen, C.Y. Chiu, CRISPR–Cas12-based detection of SARS-CoV-2, Nat. Biotechnol. 38 (7) (2020) 870–874.